Calculation of D/XB Values of Hydrocarbon Molecules in Tokamak Edge Plasmas

Hayato KAWAZOME, Kaoru OHYA[1)], Kensuke INAI[1)], Jun KAWATA, Kenji NISHIMURA[2)] and Tetsuro TANABE[3)]

Department of Information Engineering, Kagawa National College of Technology, Mitoyo, Kagawa 769-1192, Japan
[1)]*Institute of Technology and Science, The University of Tokusihma, Tokushima, Tokushima 770-8506, Japan*
[2)]*Department of Electrical and Electronics Engineering, Numazu National College of Technology, Numazu, Shizuoka 410-8501, Japan*
[3)]*Interdisciplinary Graduate School of Engineering Science, Kyushu University, Fukuoka, Fukuoka 812-8581, Japan*

(Received 6 December 2009 / Accepted 14 April 2010)

In order to investigate the dependence of effective inverse photon-efficiency D/XB values on the plasma parameters, we have been performed calculations of effective D/XB values by Monte Carlo method. Photon fluxes are converted into particle fluxes with aid of D/XB values. A D/XB value is critical factor in the study of chemical erosion by spectroscopic measurement. In modeled tokamak edge plasma, transfer of hydrocarbon molecules (CH_4, C_2H_x(x = 2,4,6), C_3H_y(y = 4,6,8)) and CH and C_2 emissions have been simulated. The plasma temperature ranged from 1 eV to 100 eV and the plasma densities are $10^{18}\,m^{-3}$, $10^{19}\,m^{-3}$ and $10^{20}\,m^{-3}$. In the temperature region of less than 3 eV, the calculated D/XB values increase with decreasing temperature due to decreasing of emission counts. In the high temperature region ($\geq$ 10 eV), the D/XB values increase with a rise in the temperature due to decrease of number of fragment of type CH and C_2.

Keywords: Plasma wall interaction, Chemical erosion, Hydrocarbon, Spectroscopy, Computer simulation

DOI: 10.1585/pfr.5.S2073

1. Introduction

Carbon-based material is one of the most widely used materials for a divertor plate and wall of magnetically confined fusion devices. In a next-step device, such as ITER, for steady-state operation, it is very important to estimate lifetime of carbon plasma-facing components. Chemical sputtering reduces their lifetime and increases fuel retention via redeposition. In many recent tokamaks and plasma simulators, chemical sputtering yields are experimentally measured by spectroscopic method using inverse photon-efficiency D/XB [1–6], where D describes the decay rate coefficient of hydrocarbon molecule into CH or C_2 and, X and B denotes the excitation rate coefficient from ground state into the electronically excited state and the branching ratio of the observed transition, respectively. In this calculation, the coefficient D is determined by not only plasma parameters but also reflection and redepositon processes on a wall and particle transport. Therefore, we describe D/XB as effective D/XB in this study. Photon fluxes are converted into particle fluxes with aid of effective D/XB values. For example, methane particle flux Γ_{CH_4} are determined from photon flux of CH emission I_{CH} according to $\Gamma_{CH_4} = D/XB \times I_{CH}$ [7]. Effective D/XB values are critical factors in the study of chemical erosion by spectroscopic measurements. In this study, effective D/XB values of hydrocarbon molecules for CH and C_2 emissions have been calculated by a Monte Carlo simulation. The hydrocarbon molecules taken into account in this study are methane (CH_4), ethane family (C_2H_2, C_2H_4, C_2H_6) and propane family (C_3H_4, C_3H_6, C_3H_8). In simple modeled tokamak divertor plasma region with the constant plasma temperature and plasma density, hydrocarbon transport are simulated, and we have investigated plasma temperature and density dependences of D/XB values.

2. Simulation Model

In this study, effective D/XB values have been calculated by the Monte Carlo simulation code, which is developed in the University of Tokushima [8]. The complex dissociation and ionization reactions of hydrocarbon molecules and the surface reflection process are taken into account. The reaction processes included in the model are (a) ionization and dissociative ionization by electron impact, (b) dissociation by electron impact, (c) dissociative recombination and (d) charge exchange with hydrogen (deuterium) ions. The rate coefficients for reactions (a) - (d) are referred from data set of Janev and Reiter [9, 10]. Reflection coefficients of all of the dissociation products on the surface are evaluated by a classical molecular dynamics simulation [11]. Hydrocarbon molecule ions, which are produced by the reaction with ionization process, gy-

author's e-mail: kawazome@di.kagawa-nct.ac.jp

rate due to the Lorentz force and move along the direction parallel to the magnetic field lines due to a force $F_{\parallel}$. The parallel force $F_{\parallel}$ consists of friction and thermal gradient force. In the simulation, the plasma flow is assumed to be no reversal flow and thus friction force is directed toward the divertor plate. The thermal gradient force makes impurity ions move to the upstream direction. The friction force and thermal gradient force increase with increasing plasma density and with increasing plasma temperature, respectively.

Figure 1 shows a schematic diagram of the modeled divertor plasma and simulation volume [8]. The simulation volume has a size of $10 \times 10 \times 10\,\mathrm{cm}^{-3}$. The angle of the magnetic field lines with the toroidal direction is 5 degree and the lines are inclined by 60 degree against the poloidal direction. The magnetic field strength is 5 T. The hydrocarbon molecules are released at the center of the divertor plate with a Maxwellian velocity distribution corresponding to a temperature of 0.1 eV (1160 K). The released particle number is 10^5. The transport of launched hydrocarbon molecules is calculated until they leave the simulation volume or redeposit on the divertor plate. The launched particles reside in the simulation volume for $1 \times 10^{-7} \sim 5 \times 10^{-6}$ s, typically.

Emission intensities of CH (transition: $A^2\Delta - X^2\Pi$, $v = 0 - 0$, Gerö band with a band head at 431 nm) and C_2 (transition: $d^3\Pi_g - a^3\Pi_u$, $v = 0 - 0$, Swan band with a band head at 516.5 nm) are calculated in a condition of a corona equilibrium. Dissociative recombination is one of important excitation processes to the A state of CH, and the calculation of the emission intensity require consideration of this excitation process. But because it is too difficult to calculate the rate coefficient of this process, excitation caused by dissociative recombination is not taken into account in this study. For CH and C_2 emissions, exitation rate coefficients calculated with IPProg code are used [12]. In many experiments, because the intensities of the CH/CD band emission are defined as emission integrated over a few wavelength width from the band head of the transition (0-0), emissions of transitions (1-1) and (2-2) are also integrated. But, in this study, we calculate the emission of transition (0-0) only. The vibrationally resolved excitation rate coefficients are 1.48 larger than the non-vibrationally resolved ones [13], and thus calculated emission counts for CH A-X band are multiplied by factor 1.48. The inverse photon-efficiency is obtained by taking the ratio of the number of the launching hydrocarbon molecules to the photon emission events of CH or of C_2 .

3. Result and Discussion

Figure 2 shows calculated effective D/XB of the CH emission from CH_4 at the plasma densities of 10^{18}, 10^{19} and $10^{20}\,\mathrm{m}^{-3}$. In the figure, experimental values are also shown. At all of plasma densities, the effective D/XB values decrease with increasing temperature up to 3 eV and then these increase with the temperature caused by decrease of number of hydrocarbon fragment of type CH, which are produced by dissociation processes. A similar dependence is obtained in the ERO calculation for the CH emission [14] and steady-state solution of a set of reaction equations [15]. In the Ref. [14], D/XB values are calculated in the homogenous plasma with constant temperature and density. In addition, electrical fields and diffusion and friction forces are not taken into account. The calculated effective D/XB values are a few times larger than that of the ERO calculation. On the other hand, in the Ref. [15], at plasma density of $1 \times 10^{20}\,\mathrm{m}^{-3}$ and the residence time of neutral molecules of infinity ($\tau_{\mathrm{neutrals}} = \infty$), there is a good agreement with the calculated D/XB values up to 30 eV in the case of $\tau_{\mathrm{ions}} = 1 \times 10^{-6}$ s. In comparison with the D/XB values observed in different fusion devices, the effective D/XB values for the temperature over 20 eV are

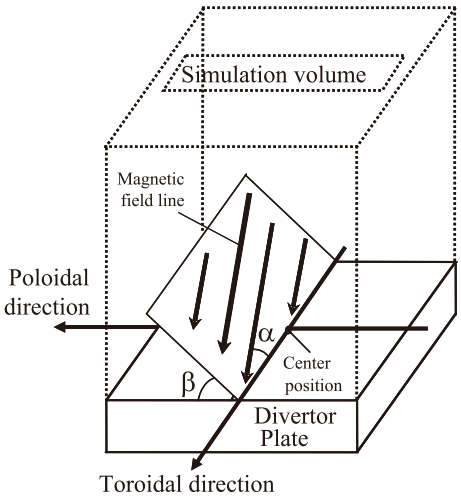

Fig. 1 The schematic diagram of the modeled divertor plasma and simulation volume [8].

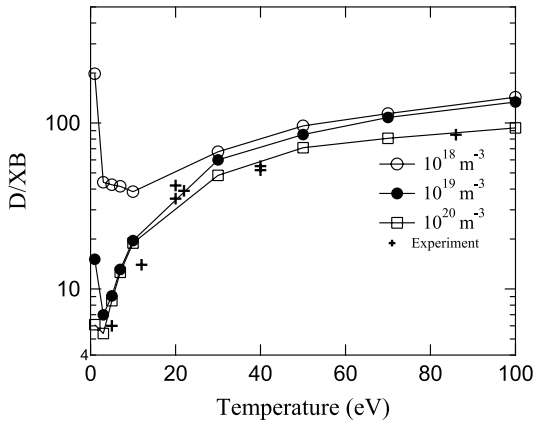

Fig. 2 Temperature dependence of effective D/XB of the CH emission from CH_4 at the plasma densities of 10^{18}, 10^{19} and $10^{20}\,\mathrm{m}^{-3}$. Experimental values in different fusion devices are also shown.

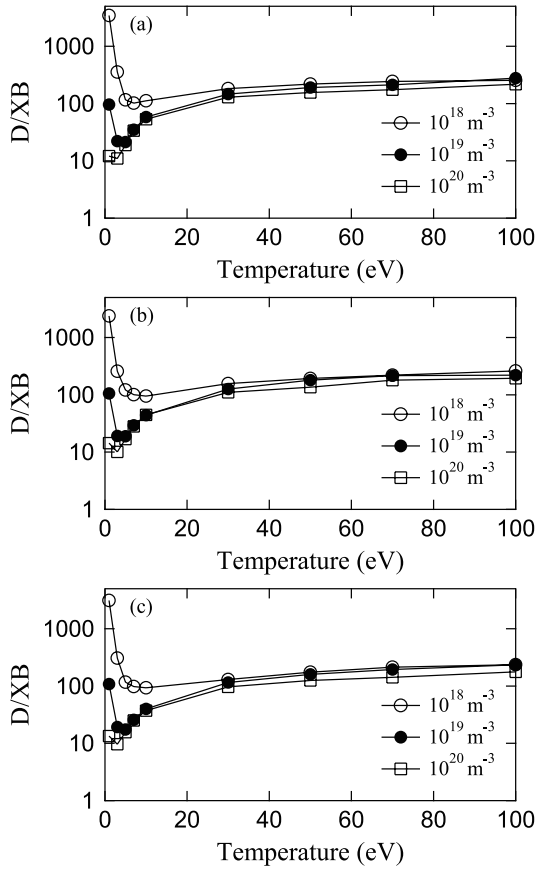

Fig. 3 Temperature dependence of effective D/XB of the CH emission from (a) C_2H_2, (b) C_2H_4 and (c) C_2H_6 at the plasma densities of 10^{18}, 10^{19} and 10^{20} m^{-3}.

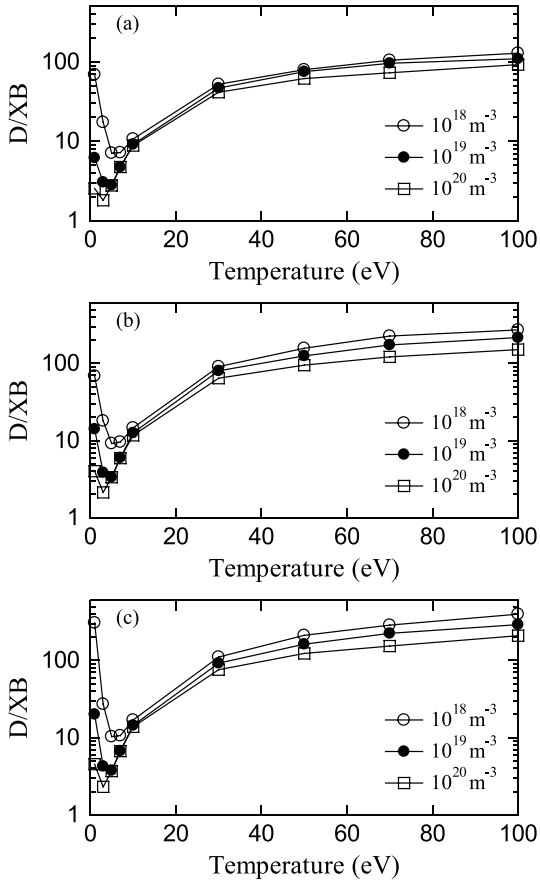

Fig. 4 Temperature dependence of effective D/XB of the C_2 emission from (a) C_2H_2, (b) C_2H_4 and (c) C_2H_6 at the plasma densities of 10^{18}, 10^{19} and 10^{20} m^{-3}.

in good agreement with experimentally determined values (DIII-D [16], JET [6,17], TEXTOR [13]). For the low temperature region less than 20 eV, in the case of plasma densities of 10^{19} and 10^{20} m^{-3}, the effective D/XB values are greater than experimental values by a factor of ~ 2 [18]. In the case of plasma density of 10^{18} m^{-3}, the effective D/XB values are also greater than experimental values and differ by one orders of magnitude.

Because the effective D/XB value is obtained by dividing the released particle number by photon emission events, the D/XB value increases with decreasing photon emission events. In coronal model, emission event is proportional to the product of the excitation rate coefficient and ground state density of CH molecule. In low temperature region, the calculated D/XB values increase due to decreasing of the photon emission events, which is caused by decreasing of the excitation rate coefficient and CH molecule number. In low temperature under about 6 eV, dominant process contributing to a loss event of CH_4 molecule is charge exchange ionization with hydrogen ions. For example, when the temperature is 1 eV, the rate coefficient of electron impact dissociation D_{CH_4} and of electron impact ionization S_{CH_4} are three and five orders of magnitude less than that of charge exchange ionization CX_{CH_4}, respectively ($CX_{CH_4} \sim 10^{-9}$ m^3/s, $D_{CH_4} \sim 10^{-12}$ m^3/s, $S_{CH_4} \sim 10^{-14}$ m^3/s). The temperature dependence of the rate coefficients holds true for other methane family fragments of type CH_x ($x \leq 3$). As a result, number of the break-up product decreases. The excitation rate coefficients at 1 eV and 3 eV are 7.4×10^{-16} m^3/s and 3.5×10^{-15} m^3/s, respectively. At the density of 10^{18} m^{-3}, the D/XB values at 1 eV and 3 eV are 198.0 and 43.9, respectively. The ratio of the D/XB values 198/43.9 = 4.5 is comparable with the reciprocal ratio of the excitation rate coefficients $3.5 \times 10^{-15}/7.4 \times 10^{-16}$ = 4.7. On the other hand, at the density of 10^{19} and 10^{20} m^{-3}, the ratio of the D/XB values are 15.1/9.1 = 1.7 and 6.1/8.5 = 0.72, respectively, and emission event do not vary linearly with the excitation rate coefficient. These results are caused by increase of additional emission events from reflected molecules at the divertor plate [11]. The friction force, which toward the divertor plate, at the plasma density of 10^{18} m^{-3} is smaller than these at the plasma density of 10^{19} and 10^{20} m^{-3}. Thus, the penetration depth of hydrocarbon molecules increase with decreasing plasma density. In addition, the reflection frequency at the divertor plate increase with increasing plasma density, and so the increasing of the reflection frequency at the divertor causes decreae of the D/XB value due to the photon emission from reflected molecules.

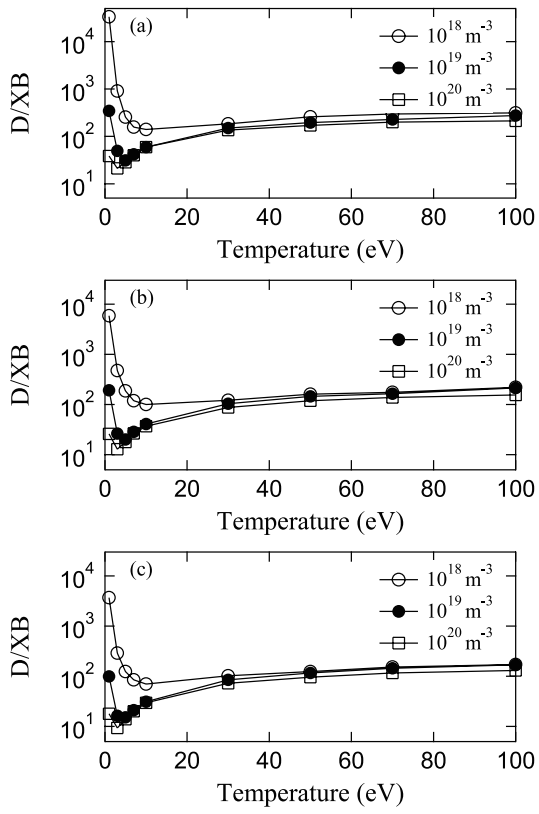

Fig. 5 Temperature dependence of effective D/XB of the CH emission from (a) C_3H_4, (b) C_3H_6 and (c) C_3H_8 at the plasma densities of 10^{18}, 10^{19} and 10^{20} m^{-3}.

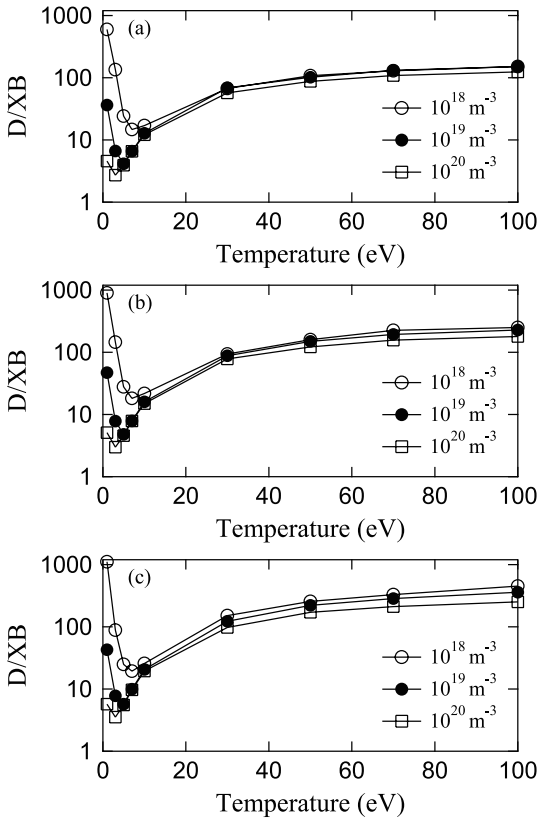

Fig. 6 Temperature dependence of effective D/XB of the C_2 emission from (a) C_3H_4, (b) C_3H_6 and (c) C_3H_8 at the plasma densities of 10^{18}, 10^{19} and 10^{20} m^{-3}.

At the plasma densities of 10^{18}, 10^{19} and 10^{20} m^{-3}, Fig. 3 and Fig. 4 show the calculated effective D/XB values of the CH emission and C_2 emission from C_2H_2, C_2H_4 and C_2H_6, respectively. In the figures, the plasma temperature dependence and plasma density dependence of the effective D/XB values are similar to that of the CH emission from CH_4 (see Fig. 2). In the comparison with experimental values, which are measured in a plasma simulator, from C_2H_2 and C_2H_4 [4], for the effective D/XB values of the CH emission, a good agreement is obtained between the experimental values and calculated values at the plasma temperature of greater than 20 eV, the D/XB values ~ 200. For the C_2 emission, the calculated values are smaller than the observation by one orders of magnitude, ~ 1000 from the experiment and ~ 200 from the calculation. In the comparison with experimental values measured in a tokamak device [19], the calculated values of the C_2 emission from C_2H_4 are in a good agreement with measured values at the temperature region greater than 20 eV. For the D/XB values of the C_2 emission from C_2H_6, the experimental values are a few times greater than calculated values, ~ 400 - 600 from the experiment and ~ 200 from the calculation.

At the plasma densities of 10^{18}, 10^{19} and 10^{20} m^{-3}, Fig. 5 and Fig. 6 show the calculated effective D/XB values of the CH emission and C_2 emission from C_3H_4, C_3H_6 and C_3H_8, respectively. In the figures, dependences of the effective D/XB values of the CH and C_2 emissions from propane family on the plasma temperature and density are also similar to these from methane and ethane family. At the plasma temperature of about 50 eV, the effective D/XB values of the CH emission and that of the C_2 emission reach about 100 and then remain almost constant. For the effective D/XB values from propane family, it is important to compare experimental values with calculated values, and experimental measurement of D/XB values is necessary.

4. Summary

In the tokamak edge plasma, the transport of hydrocarbon molecules is simulated by Monte Carlo method, and the calculations of the effective D/XB values of the CH and the C_2 emissions from hydrocarbon molecules are performed. The effective D/XB values decrease with increasing the temperature up to 3 eV. Then these increase with the temperature due to decrease of number of fragment of type CH and C_2, which is caused by increase of number of loss-event. The increasing of the friction force due to increasing of the plasma density causes the increasing of reflection frequency. As a result, the D/XB values decreases with the plasma density. For the D/XB values of the CH emission from CH_4, good agreements with other simulation results and with experimental results are obtained. For the D/XB

values from ethane and propane families, detailed comparisons with experimental results are necessary and will been performed in the future work.

Acknowledgments

This work was supported by the Ministry of Education, Science, Sports and Culture, Grant-in-Aid for Scientific Research on Priority Areas (No. 20049007).

[1] M. Balden and J. Roth, J. Nucl. Mater. **280**, 39 (2000).
[2] T. Nakano *et al.*, Nucl. Fusion **42**, 689 (2002).
[3] A. Cambe *et al.*, J. Nucl. Mater. **313-316**, 364 (2003).
[4] A. Pospieszczyk *et al.*, UCLA-PPG-1251 (Univ. of California at Los Angeles, 1989).
[5] D. G. Whyte *et al.*, Nucl. Fusion **41**, 47 (2001).
[6] M. F. Stamp *et al.*, Phys. Scr. **T91**, 13 (2001).
[7] A. Pospieszczyk *et al.*, J. Nucl. Mater. **145-147**, 574 (1987).
[8] K. Inai and K. Ohya, Jpn. J. Appl. Phys. **46**, 1149 (2007).
[9] R. K. Janev and D. Reiter, Rep. Forschungszentrum Jülich, Jül-3966 (2002).
[10] R. K. Janev and D. Reiter, Rep. Forschungszentrum Jülich, Jül-4005 (2003).
[11] K. Ohya *et al.*, J. Plasma Fusion Res. Series, in press.
[12] U. Fantz *et al.*, J. Nucl. Mater. **337-339**, 1087 (2005).
[13] S. Brezinsek *et al.*, J. Nucl. Mater. **363-365**, 1119 (2007).
[14] A. Kirschner *et al.*, J. Nucl. Mater. **313-316**, 444 (2003).
[15] D. Naujoks *et al.*, J. Nucl. Mater. **266-269**, 360 (1999).
[16] M. Groth *et al.*, J. Nucl. Mater. **363-365**, 157 (2007).
[17] S. Brezinsek *et al.*, Phys. Scr. **T111**, 42 (2004).
[18] A. Huber *et al.*, Phys. Scr. **T111**, 101 (2004).
[19] T. Nakano *et al.*, ITPA DSOL Meeting, Univ. of Toronto, Canada, Nov. 6-7, 2006.